

3. Numerical Calculations and Stability Analysis

3.1 Numerical Simulation of Three Dimensional Oscillatory Flow in Half-Zone Bridges of Low Pr Fluids

Nobuyuki Imaishi

Kyushu University

NUMERICAL SIMULATION OF THREE DIMENSIONAL OSCILLATORY FLOW IN HALF-ZONE BRIDGES OF LOW Pr FLUIDS

Nobuyuki Imaishi*, Shouich Yasuhiro* and Shinichi Yoda**

*Institute of Advanced Material Study, Kyushu University, Kasuga, 815-8580

**NASDA, Sengen 2-1-1, Tsukuba 305-8505

ABSTRACT A set of numerical simulations was conducted to understand characteristics of oscillatory Marangoni convection in half-zone liquid bridges with various aspect ratios (from 1 to 1.8) and Prandtl numbers (from 0 to 0.02) by a finite difference method. The simulation results indicated that under smaller temperature differences the flow in the liquid bridge is axisymmetric but it becomes unstable against a three dimensional disturbance beyond a certain threshold value of temperature difference. The flow becomes steady three dimensional. This steady flow becomes unstable against time dependent three dimensional disturbances beyond a second critical condition. The numerical simulations revealed the critical conditions and flow structures. The first critical conditions showed good agreements with those of linear stability analyses. The second critical conditions also agreed with previous values and gave new critical values for different conditions.

Keywords: Marangoni flow, Oscillatory flow, Critical Marangoni number, Low Pr fluid

1. INTRODUCTION

In a half-zone liquid bridge of radius a and length L , a transition from an axisymmetric to a three-dimensional (3-D) Marangoni flow takes place when the temperature difference between two solid disks exceeds a certain critical value. In the 1998 Annual Report of NASDA Marangoni Convection Modeling Research, we reported numerical simulations on 3-D oscillatory Marangoni convection in $Pr=1.02$ fluid and some preliminary results for $Pr=0.01$ and 0.02 . The early numerical study by Rupp et. al.[1] suggested that liquid bridge of low Prandtl number fluid experiences a first transition from axisymmetric to a 3-D steady flow and then at larger temperature difference the second bifurcation occurs to start oscillatory flow. Later, linear stability analyses[2-4] provided us with the critical Marangoni numbers as function of the Prandtl number, the aspect ratio ($As=L/a$) and the Biot number. Linear stability analyses indicated that 3-D Marangoni flow is always oscillatory in liquid bridges of high Pr fluids. This has been confirmed by numerical simulations of Rupp et al,[1] and others[5,6,7,8,9]. For low Pr fluids ($Pr<0.1$), however, linear stability analysis predicts Ma_c for the first bifurcation to a steady 3-D flow. The first bifurcation in a liquid bridge of $As=1.0$, $Pr=0$ and $Pr=0.01$ was numerically confirmed by Levenstam et al.[5]. They also obtained a second critical Marangoni number above which the three dimensional oscillatory flow starts but did not show the effects of aspect ratio on flow mode. Later, Leypoldt et al.[6] conducted 3-D numerical simulation for $As=1.0$, $Pr=0$ and 0.02 . These simulations predicted a 3-D flow pattern with a two-fold symmetry in azimuthal direction, in other word, $m=2$. The present authors also conducted several numerical simulations for

bridges of $As=0.75-1.6$ of $Pr=1.02$ fluid[7] and $As=1.0, 1.2$ and 1.8 for $Pr=0.01$ and 0.02 fluids [8,9]. In our previous paper [9], we reported some strange behavior of 3-D oscillations in a liquid bridge of $As=1.2$ for $Pr=0.02$. In this paper, we slightly extended the range of As and Pr to obtain better understandings of the oscillatory Marangoni flow in half-zone of low Pr fluids. These analyses will help planning and designing apparatus for the space experiments on oscillatory Marangoni flow in half-zone liquid bridge on board the International Space Station.

2. MODEL FORMULATIONS

A standard model of half-zone liquid bridge as shown in Fig. 1 is adopted [7]. The liquid surface is assumed adiabatic, non-deformable and cylindrical. This shape is true under microgravity condition. There acts the Marangoni effect on the liquid surface. Fundamental equations are as follows.

$$\nabla \cdot \mathbf{U} = 0 \quad (1)$$

$$\partial \mathbf{U} / \partial \tau + (\mathbf{U} \cdot \nabla) \mathbf{U} = -\nabla P + \nabla^2 \mathbf{U} \quad (2)$$

$$Pr(\partial \Theta / \partial \tau + (\mathbf{U} \cdot \nabla) \Theta) = \nabla^2 \Theta \quad (3)$$

Initial conditions: $\mathbf{U} = 0, \quad \Theta = -0.5, \quad \tau \leq 0$

Boundary conditions:

on both end plates ($Z=0$ and As):

$$U(R, \theta, 0) = U(R, \theta, As) = 0, \quad \Theta(R, \theta, 0) = +0.5, \quad \Theta(R, \theta, As) = -0.5$$

at the surface ($R=1$):

$$\partial \Theta / \partial R = 0, \quad \partial U_z / \partial R = -Re \partial \Theta / \partial Z,$$

$$R^2 \partial (U_\theta / R) / \partial R = -Re \partial \Theta / \partial \theta, \quad U_R = 0.$$

These equations are equivalent to those reported last year. But slightly different definitions of non-dimensional variables are adopted as follows in order to enable simulations on $Pr=0$ fluid. The dimensionless parameters are the Prandtl number, the Reynolds and the Marangoni numbers defined as $Pr = \nu / \alpha$, $Re = \sigma_T \Delta T a / \mu \nu$ and $Ma = \sigma_T \Delta T a / \mu \alpha = Re Pr$, respectively. The non-dimensional variables are defined as; $\{R, Z\} = \{r/a, z/a\}$, $P = pa^2 / (\nu \mu)$, $U = ua / \nu$, $\Theta = (T - T_m) / \Delta T$, $\tau = t \nu / a^2$, where $T_m = (T_h + T_c) / 2$, $\alpha = \lambda / c_p \rho$, u : velocity, p : pressure, c_p : heat capacity, ρ : density, λ : thermal conductivity, μ : viscosity and ν : kinematic viscosity.

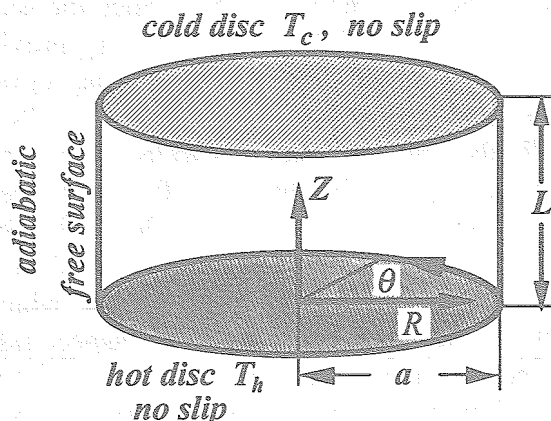


Fig.1 Model of a half-zone liquid bridge.

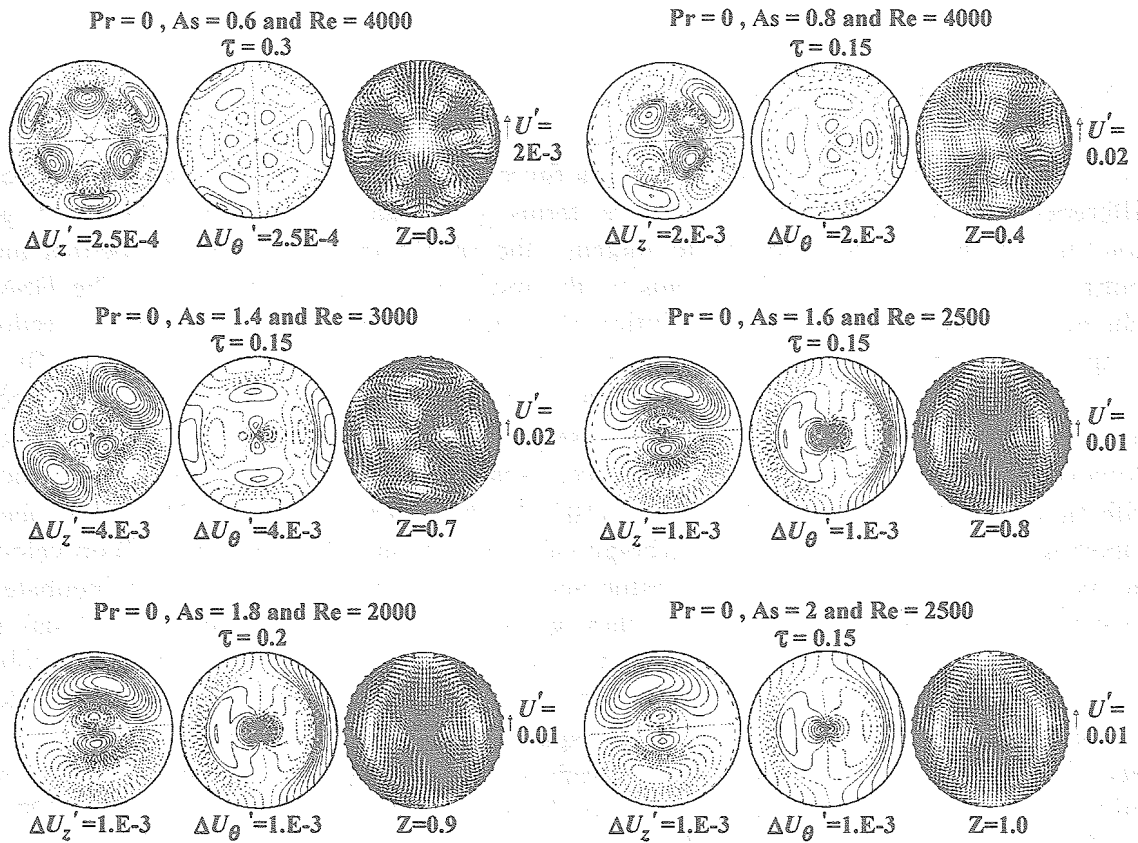


Fig.3 Snap-shots of growing small disturbances at very early stage in bridges of $As=0.6-2.0$.

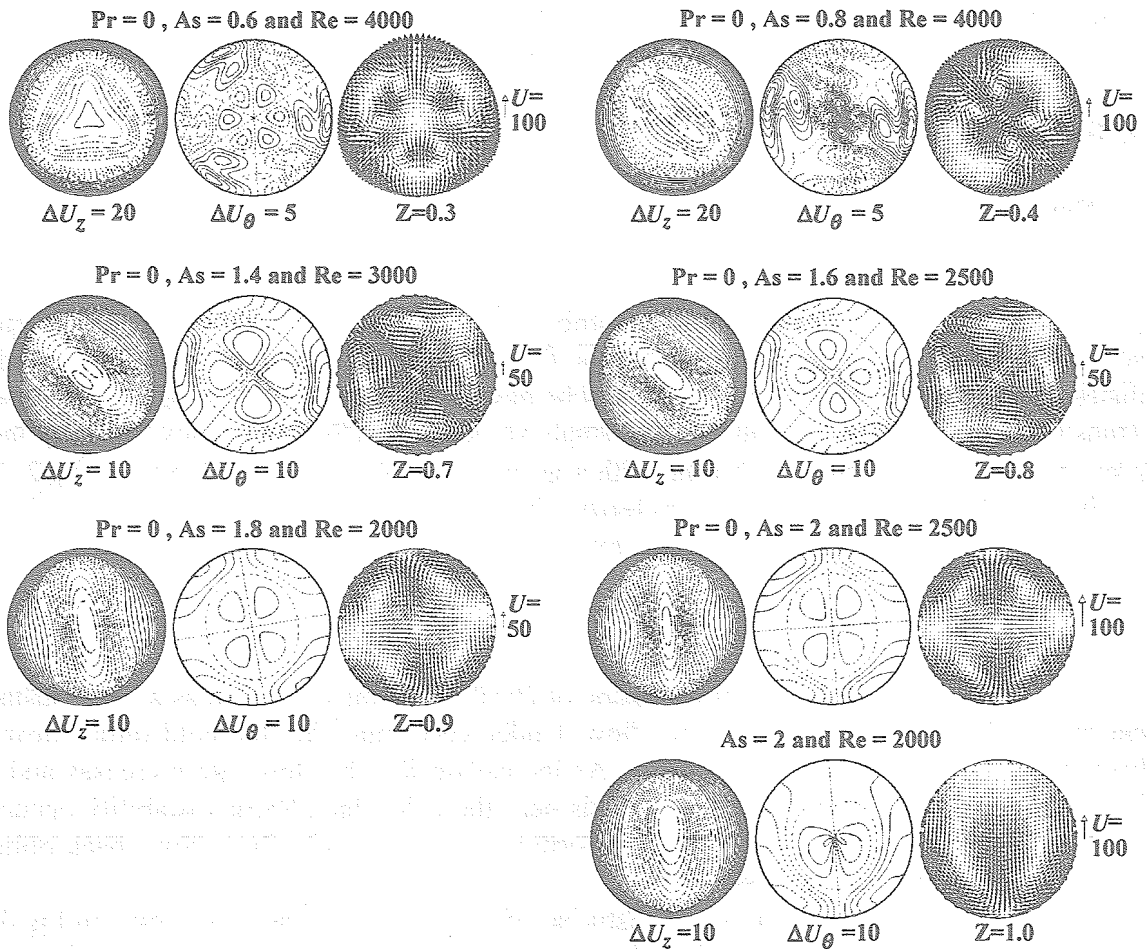


Fig.4 Snap-shots of 3-D steady flow in bridges of $As=0.6-2.0$.

3. NUMERICAL METHOD

These equations are discretized by a finite difference method with a modified central difference treatment for the convective terms [10] and non-uniform staggered grids. Non-uniform grids were adopted to increase the resolution. The radial velocities on the central axis were calculated by means of the method of Ozoe et al. [11]. The HSMAC scheme was used to proceed time evolution of velocity and pressure. For the sake of reducing computation time, the energy equation was solved by an implicit method. By this modification, computation speed was increased by a factor of 3 to 10. This method becomes more effective for smaller Pr cases. Time step $\delta\tau$ was chosen between 1×10^{-5} and 1×10^{-4} . However, the critical Reynolds numbers were searched by means of fully explicit method with time step $\delta\tau$ between 1×10^{-6} and 5×10^{-6} . In this work, we gave 3-D disturbances by imposing very small random value (average value=0, standard deviation of 10^{-8}) on velocities on every grid points, as embryos of disturbance. These numerical disturbances incubate 3-D disturbances automatically and they start growth with time. A two dimensional (2D) simulation code with the same scheme and 2D grids was run in order to obtain a 2D solution under the same conditions. If we adopt thermophysical properties of molten silicon, such as $\nu = 2.5 \times 10^{-7}$ [m^2/s], non-dimensional time span $\Delta\tau = 1$ corresponds approximately to 100 seconds for a liquid bridge of 5.0mm in radius. The program was run on an MPU of the Fujitsu VPP700 at the Computer Center of Kyushu University or Compaq XP-1000. The validity of the numerical code has been reported for $Pr = 1.02$ fluid [7] and also for $Pr = 0.01$ fluid^{8,9)} by comparing the first critical Reynolds numbers (Re_{c1}) with those of linear stability analyses[3,4], and also comparing the second critical Reynolds numbers (Re_{c2}) with available results [5,6,12]. By our code, we determined both the first and the second critical Reynolds numbers within few percent of error from the reported values.

4. RESULTS

4.1 Results with $Pr = 0$

4.1.1 Steady 3-D flow and Re_{c1}

As for a limit of the small Pr number cases, a set of simulations was conducted by setting $Pr = 0$. In this case, the Marangoni flow is induced by a linear axial temperature distribution but the temperature field would be never disturbed by any change of flow pattern. Transient numerical simulations with a small value of Re ($Re > Re_{c1}$) shows an exponential growth of 3-D disturbance with time with a growth rate constant β as shown in Fig.2. Mode of the 3-D Marangoni flow is characterized by the azimuthal wave number, m . Then, the growth process of disturbance would be expressed as:

$$X(\tau) = X(0) \sin(m\theta) \exp(\beta\tau)$$

Origin of the 3D flow in half-zone of $Pr = 0$ fluid was explained as a shear instability caused by the large amount of return flow. Under very small Re , the cold return flow goes back along the axis as a coaxial plume. As increasing Re , the flow rate increases and large amount of returning liquid meets at the axis near the cold plate. Shear instability occurs at a certain flow rate and the return flow is deformed oblate and cold fluid flows back obliquely and a 3-D flow pattern is formed [12].

Snap-shots of growing small disturbances at very early stage are shown in Fig.3. In a short bridge ($As = 0.6$), growing disturbance is characterized as $m = 3$ and this disturbance

continues its growth. In bridges of $As=0.8-1.4$, disturbance with $m=2$ is incubated and increases its amplitude until its steady state. In longer bridges, $As=1.6 - 2.0$, the very initial disturbances are mostly characterized as $m=1$ as shown in Fig.3. But in bridge of $As=1.6$ soon a disturbance with $m=2$ takes places and starts growing. In bridges of $As=1.8$ and 2.0 , the initial disturbance with $m=1$ survives until it grows up to a detectable 3-D steady flow. But in cases of $As=1.8$ and $As=2.0$ with $Re_{c2} > Re > 2500$, a mode shift occurs and the finally observable flow pattern is characterized by $m=2$, as shown in Fig.2 and Fig.4. Only in case of $As=2.0$ with $2000 > Re > Re_{c1}$, a 3D disturbance with $m=1$ continues its growth. In these cases, we can determine the growth rate constant β value from slope of the semi-logarithmic plot of $U_{\theta_{max}}$ vs. τ . By plotting β vs. Re as shown in Fig.5, we can determine the first critical Reynolds number which is defined as the Re value at which β crosses zero. Thus determined first critical Reynolds number, Re_{c1} , are summarized in Fig.6, as a function of aspect ratio, As .

In liquid bridges of $Pr=0$ fluid, the 3-D steady flow pattern of $m=2$ is dominant over wide range of As ($As=0.8-2.0$) except for the 3-D steady flow with $m=3$ at $As=0.6$. However, it should be noted that the most dangerous mode for $As=1.8$ and 2.0 is $m=1$. Thus determined Re_{c1} fall below those for finite Prandtl number fluids ($Pr=0.01$ and 0.02) obtained by linear stability theory [3, 4].

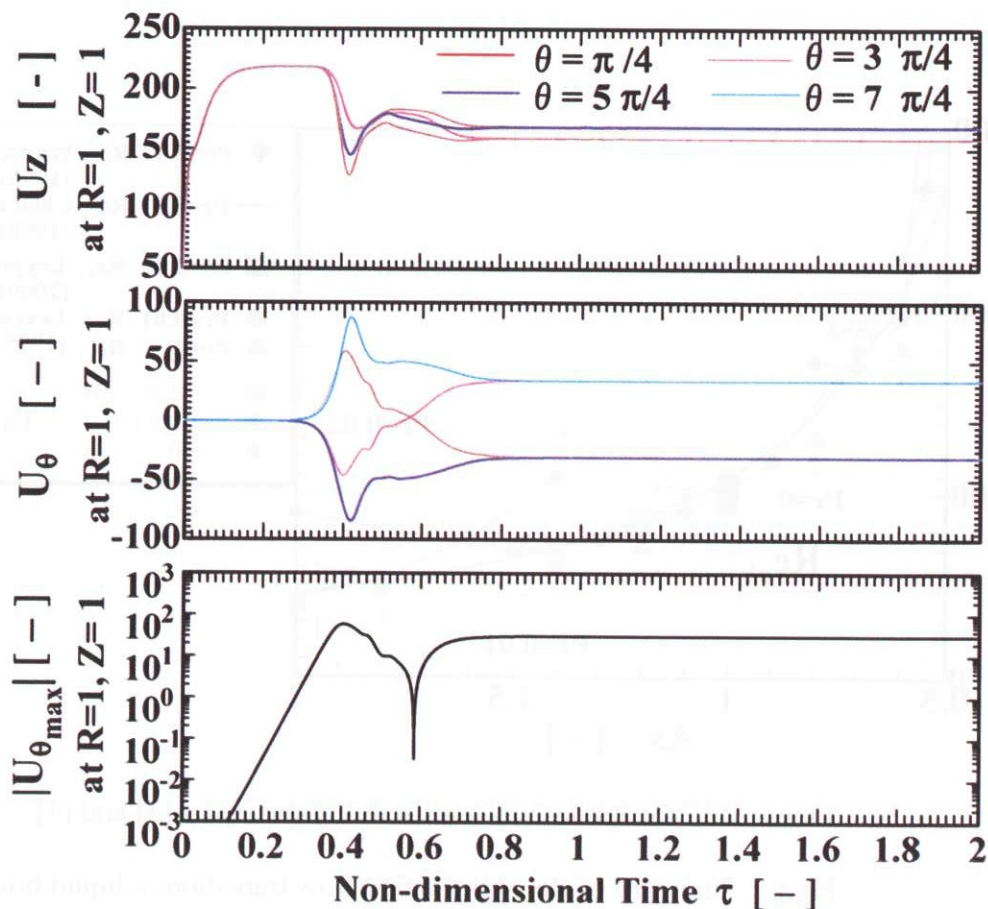


Fig.2 Time evolution of 3D Marangoni flow in a liquid bridge of $Pr=0$, $As=2$ and $Re=2500$.

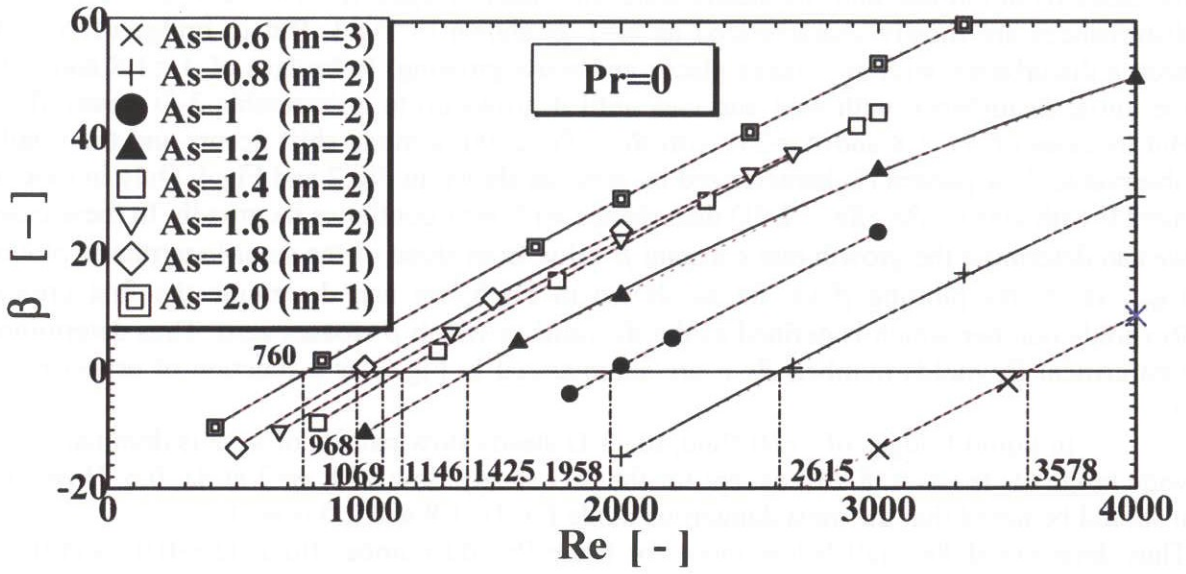
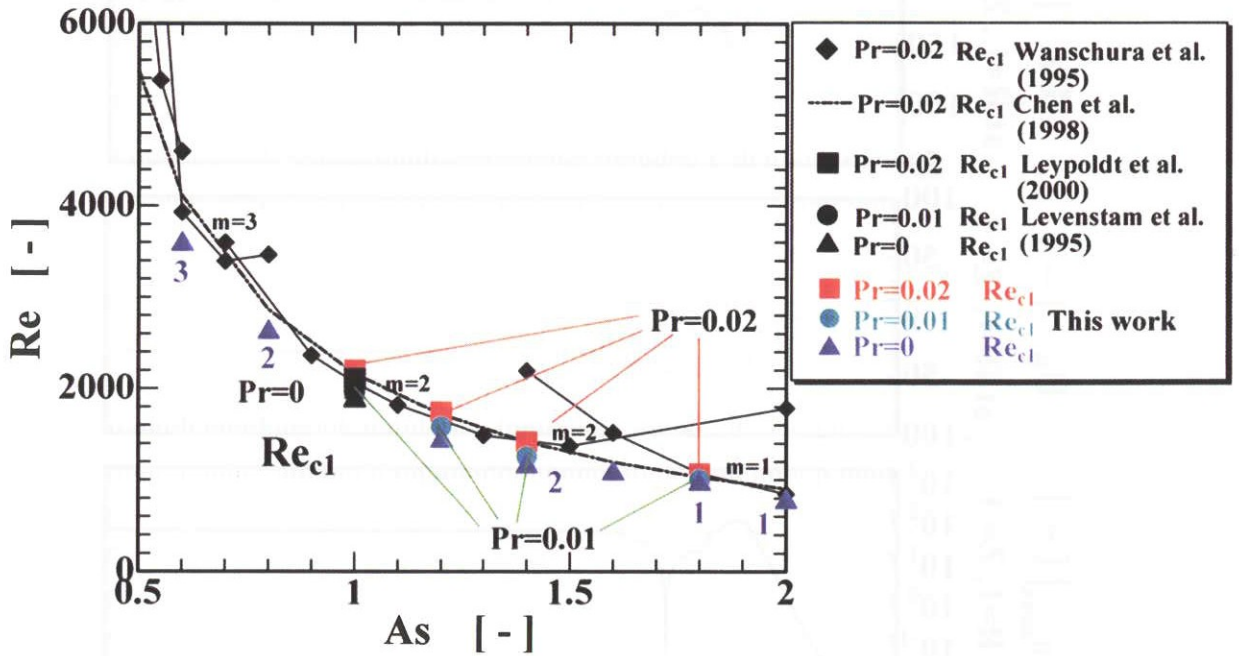


Fig.5 The β vs. Re plot to determine Re_{c1}



Lines : Re_{c1} for $Pr=0.02$ by liner stability theory by [3] and [4].

Fig.6 Summary of Re_{c1} for the first flow transition in liquid bridge of low Prandtl number fluids ($Pr=0, 0.01$ and 0.02) as a function of aspect ratio, As .

4.1.2 Oscillatory flow and second critical Reynolds number, Re_{c2}

These steady 3-D flows become unstable against time-dependent 3-D disturbances and start oscillation at and beyond the second critical Reynolds number. For example, in a liquid bridge of $As=1.4$, the 3D steady flow becomes unstable and exhibits oscillations as shown in Fig.7 at $Re=5850$. The oscillation at early stage ($\tau=0.17-0.45$) is characterized by the time-dependent disturbance of $m=1$ imposed on the basic steady flow of $m=2$, as shown in Fig.8-a. This type of oscillation is well known for short liquid bridge of low Pr fluids [5,6,8]. As time passes, this type of oscillation is taken over by a different type of oscillation at $\tau > 0.7$. The new type of oscillation is featured by the torsional-oscillating (twisting) action of the longer axis of the oblique cold plume in azimuthal direction, as shown in Fig.8-b.

Transition of oscillation mode also occurs in long liquid bridge. Fig.9 shows an example of such transition in a liquid bridge of $As=1.8$ at $Re=4000$. In the early stage, oscillation is classified as $m=2$ torsional oscillation, but Fig.10 shows that later an oscillating disturbance of $m=1$ is superimposed on the torsional oscillatory flow of $m=2$, similar to that in Fig.8-b. In much longer liquid bridges, such as $As=2.0$, the dominant mode of oscillation is the torsional oscillation. After long time, the flow cells starts drifting and the pattern get somehow distorted.

Growth and decay of the oscillation amplitude of $|U_R|$ at a point ($R=0, Z=0.5As$) with time depends on Re value as shown in Fig.11. The growth rate constant β is determined and plotted against Re . Then the second critical Reynolds number is determined from the cross-over point. Thus determined values of Re_{c2} , yet incomplete, are plotted in Fig.12 as a function of As together with Re_{c1} . It must be noted that Re_{c2} shows local maximum at $As=1.2$. The physics behind this anomaly is yet to be investigated.

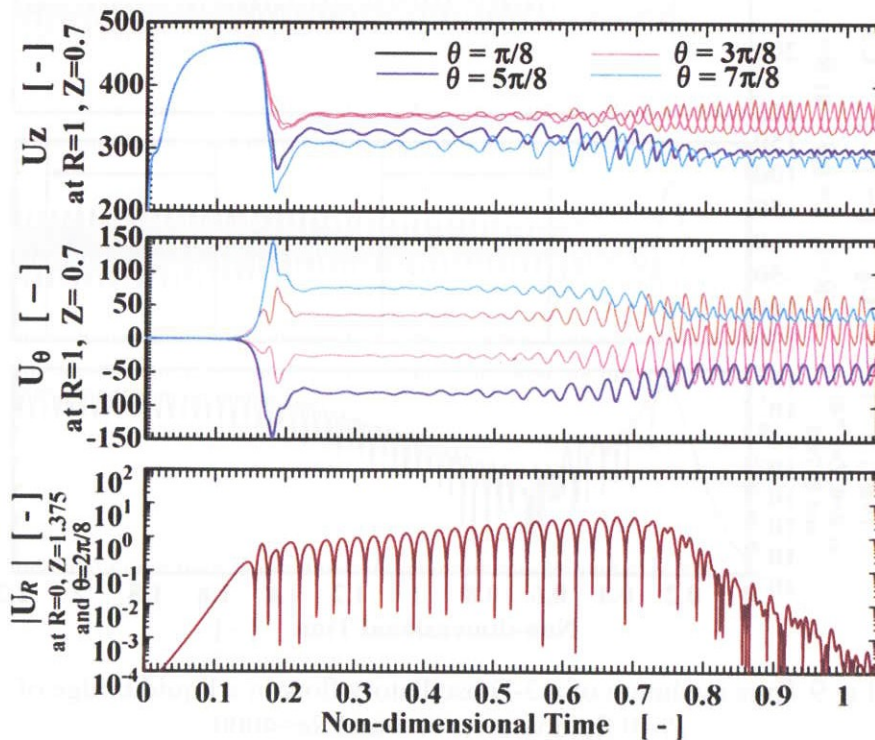


Fig.7 Time evolution of a 3-D oscillatory Marangoni flow in a bridge of $Pr=0$ fluid at $As=1.4$ and $Re=5850$.

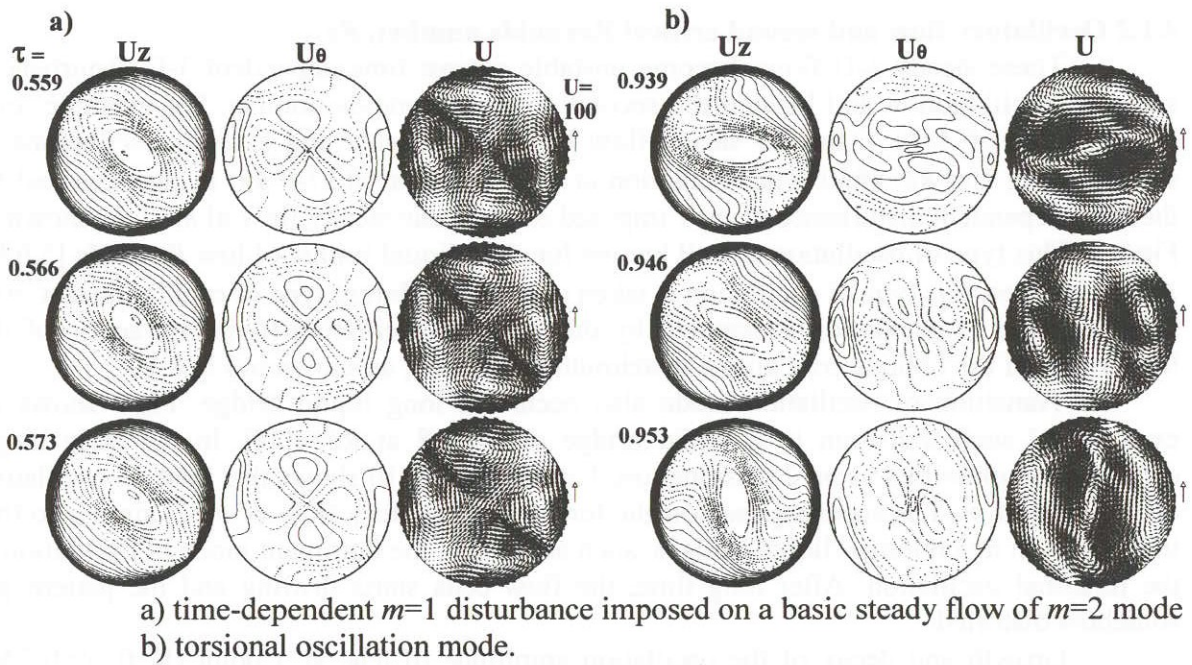


Fig.8 Snapshots of contour line of axial and azimuthal velocity, velocity vectors on $Z=0.7$ plane over a half period of oscillation in a liquid bridge of $Pr=0$ fluid at $As=1.4$ and $Re=5850$.

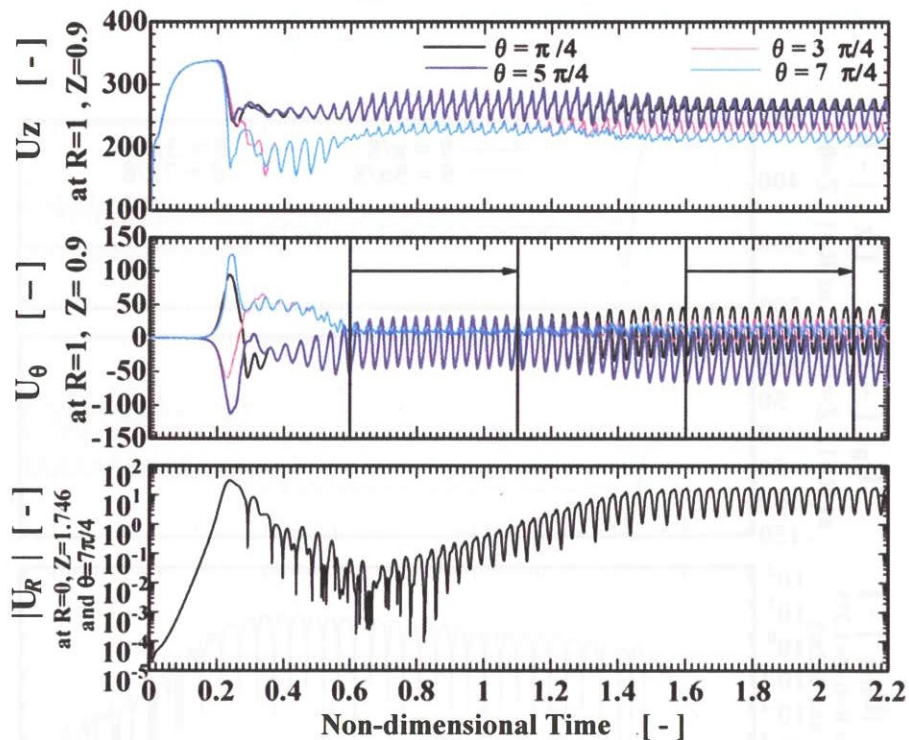


Fig.9 Time evolution of a 3-D oscillatory flow in a liquid bridge of $Pr=0$ fluid with $As=1.8$ and $Re=4000$.

$\tau = 0 - 0.3$: $m=1$ non-oscillatory. $\tau = 0.3 - 0.7$: growing pulsating oscillatory flow of $m=2$.
 $\tau = 0.7 - 1.2$: dominant pulsating $m=2$ oscillation and growth of a oscillatory $m=1$ disturbance.
 $\tau = 1.5 -$: oscillatory $m=1$ disturbance imposed on $m=2$.

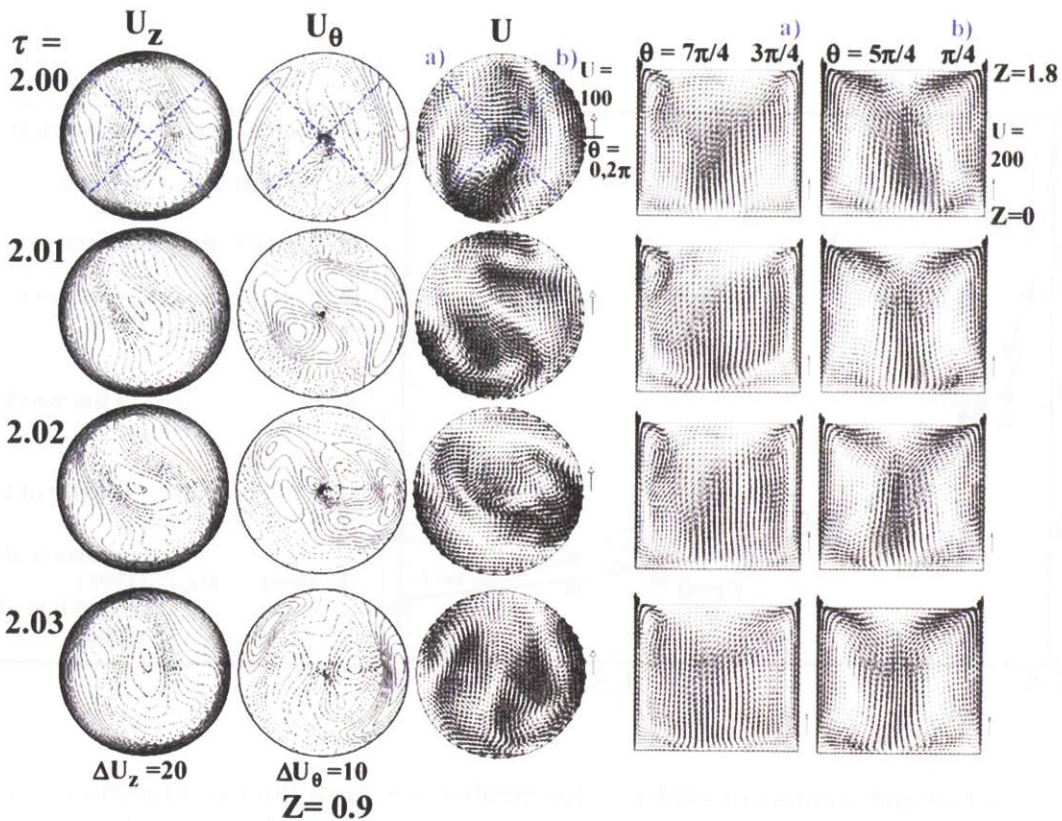


Fig.10 Snapshots of contour line of axial and azimuthal velocity, velocity vectors on $Z=0.9$ plane and velocity vectors in two vertical cut planes (a) and b) over a half period oscillation : $Pr=0, As=1.8$ and $Re=4000$.

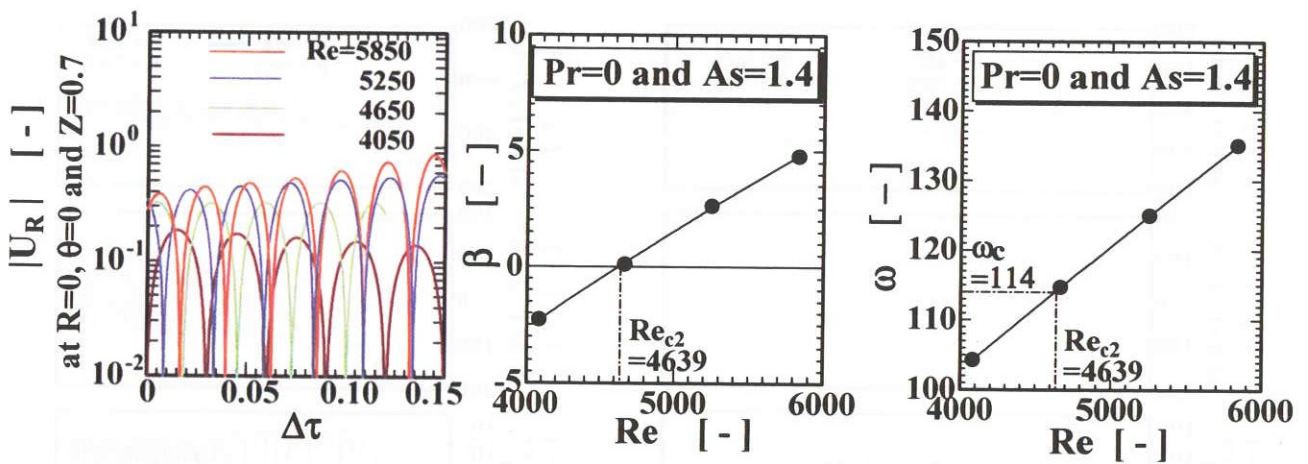


Fig. 11 Growth and decay of the oscillation amplitudes at different Re values (left) and plots of the growth rate constant β and oscillatory frequency ω as a function of Re .

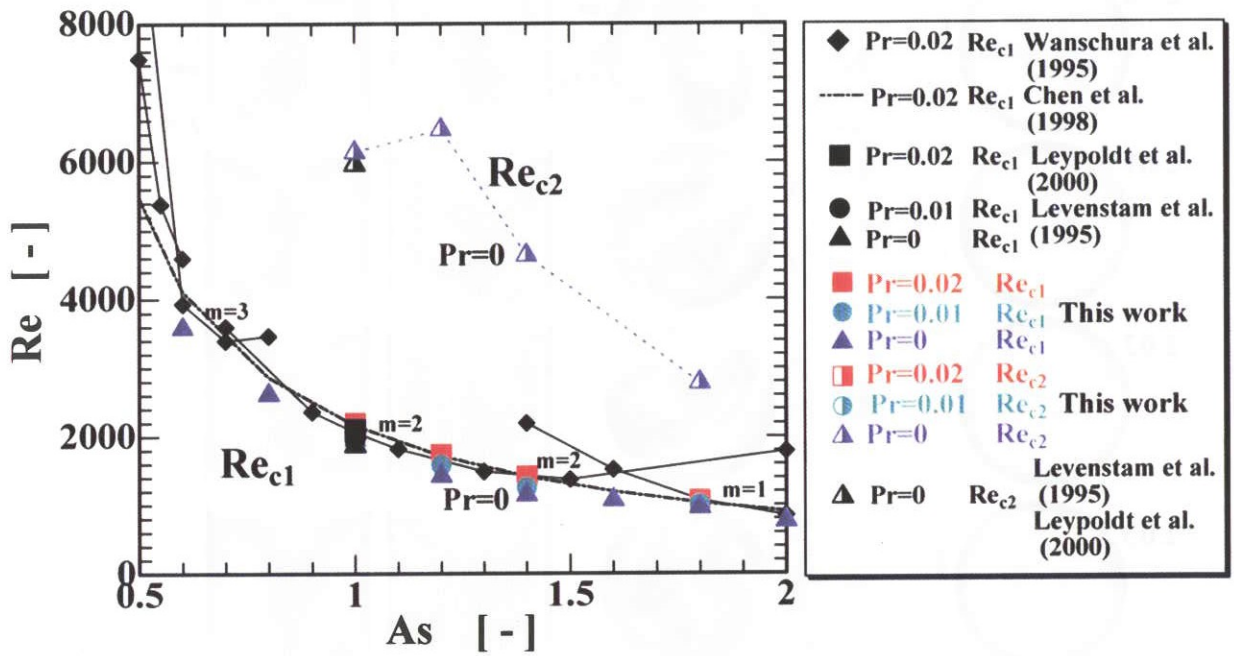


Fig.12 The first and second critical Reynolds numbers for $Pr=0$ fluid as a function of As , in comparison with the first critical Reynolds numbers for finite Pr values.

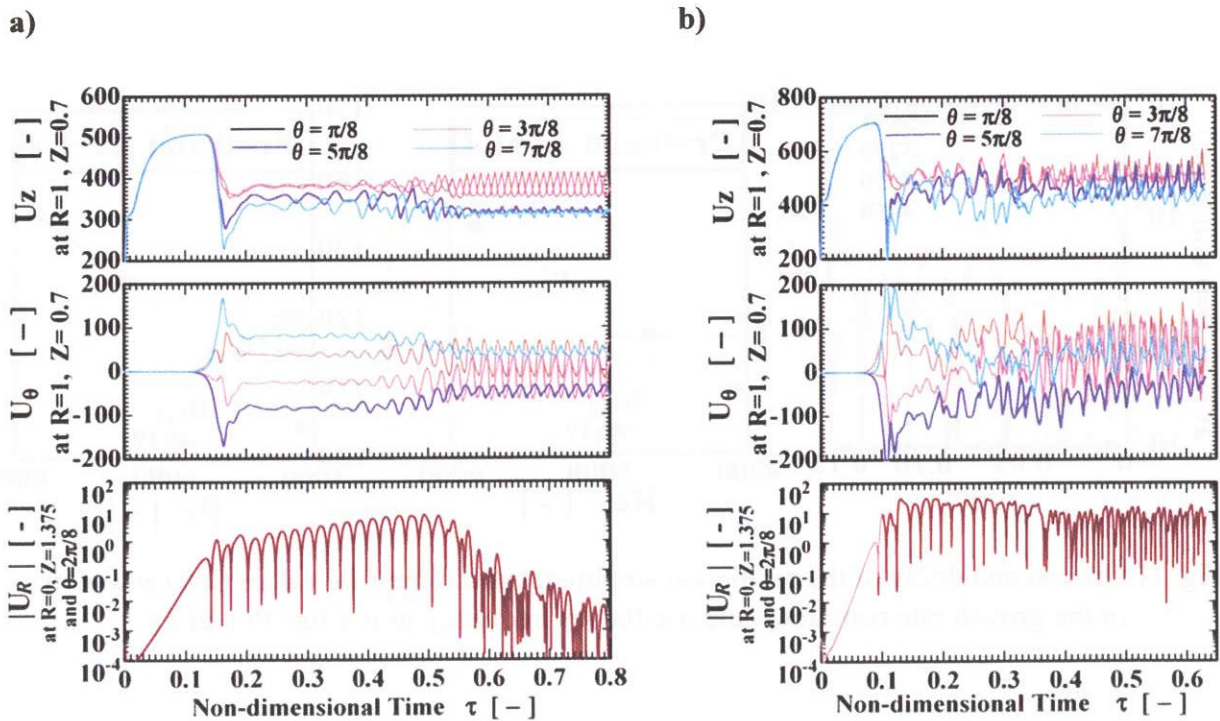


Fig. 13 Time evolution of 3-D oscillatory Marangoni flow in a liquid bridge of $Pr=0$ fluid with $As=1.4$, a) periodic oscillation at $Re=7600$ and b) random oscillations at $Re=10000$.

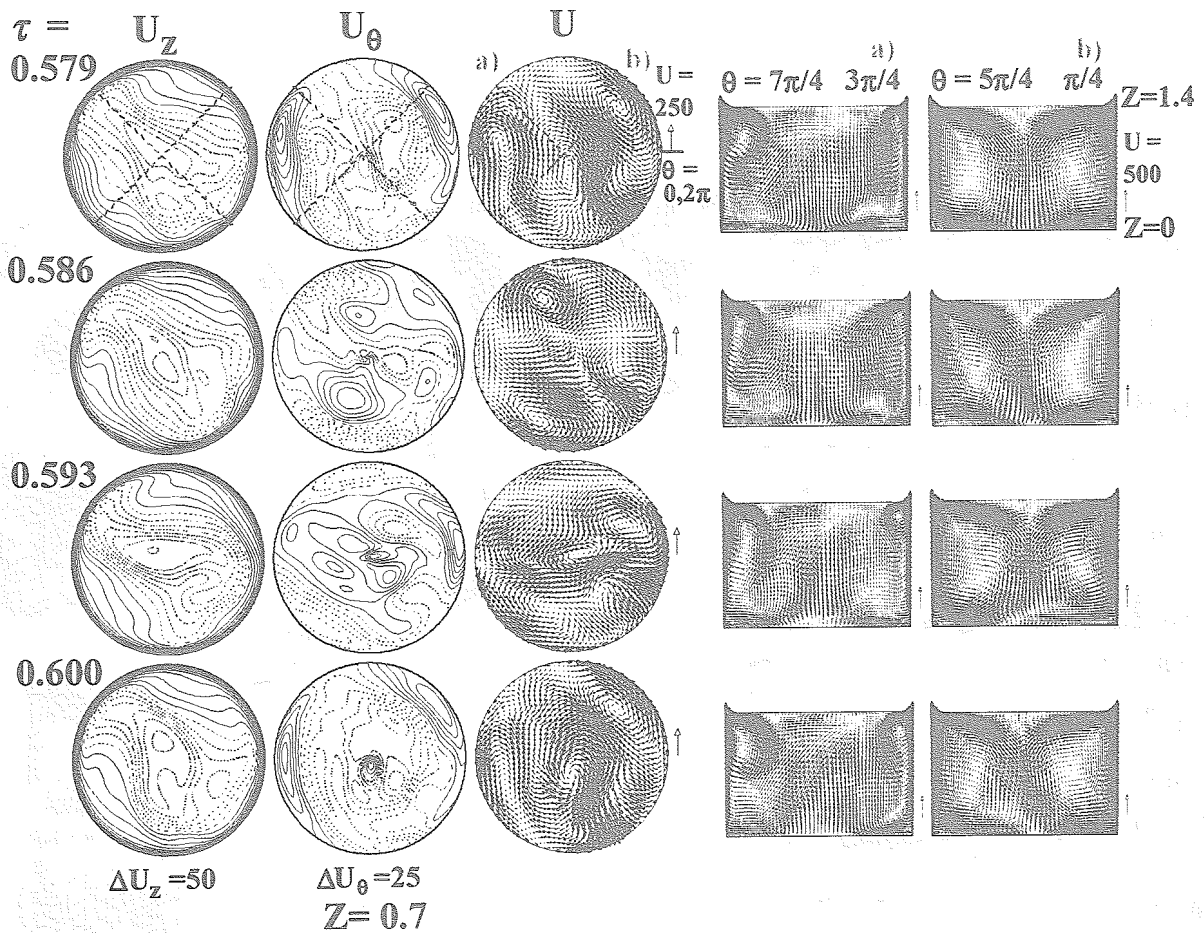


Fig.14 Snapshots of contour line of axial and azimuthal velocity, velocity vectors on $Z=0.7$ plane and velocity vectors in two vertical cut planes (a) and b)) during the random oscillations in a liquid bridge of $Pr=0$ fluid with $As=1.4$ and $Re=10000$.

The effect of Re on the oscillation behavior is shown in Fig. 13 for a bridge of $As=1.4$. By increasing Re , the oscillation period becomes shorter. At $Re=10000$, local velocities start kind of random oscillations and power spectra show broadened multi frequency peaks. These are originated by the aperiodic ejection of eddies from the shear layer, as shown in the snapshots of velocity vectors on the mid plane at $Z=0.7$: Fig.14.

4.2 Results for $Pr=0.01$

4.2.1 First transition and Re_{c1}

For $Pr=0.01$ fluid, the critical conditions for the first and the second transitions have been reported for $As=1.0$ and $As=1.2$ in previous papers [7,8,9]. In this paper, we added simulation for $As=1.4$ and 1.8 . With this small, but finite, value of Pr , a change in flow pattern may give influences on the temperature distribution and may cause the Marangoni effect in azimuthal direction. In half zones with $As=1.0-1.8$, the steady 3-D flow is classified to $m=2$, as shown in Fig.15 for $As=1.8$. This suggests that the coupling between flow field and temperature field is not so much significant in these conditions. The growth rate constant β is used to determine the first critical Reynolds number, Re_{c1} . The results are plotted in Fig.5. The present result at $As=1.0$ agrees well within 6% of error with that of Levenstam et al [5]. Present results of Re_{c1} for $Pr=0.01$ fall slightly above the results for $Pr=0$.

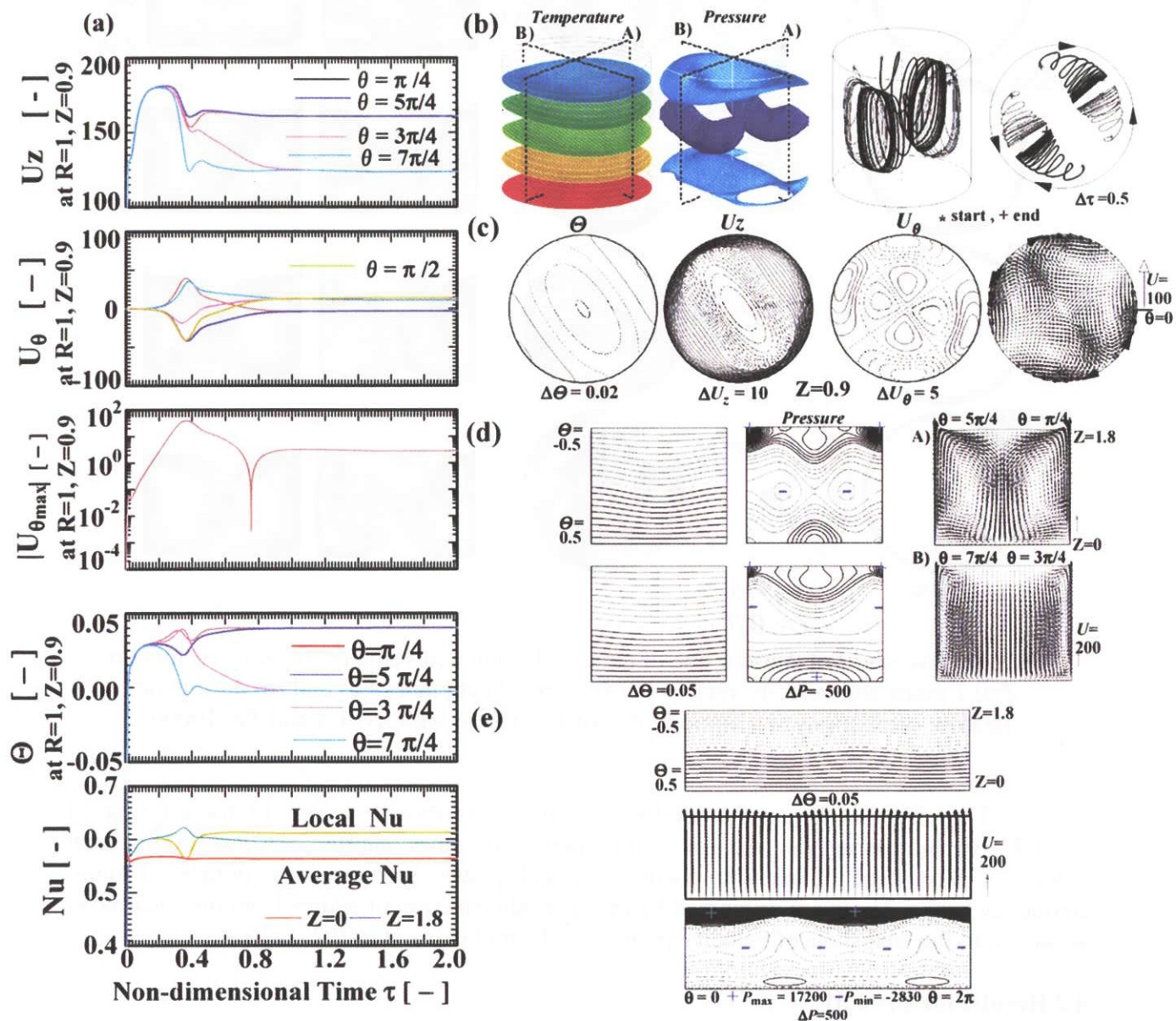
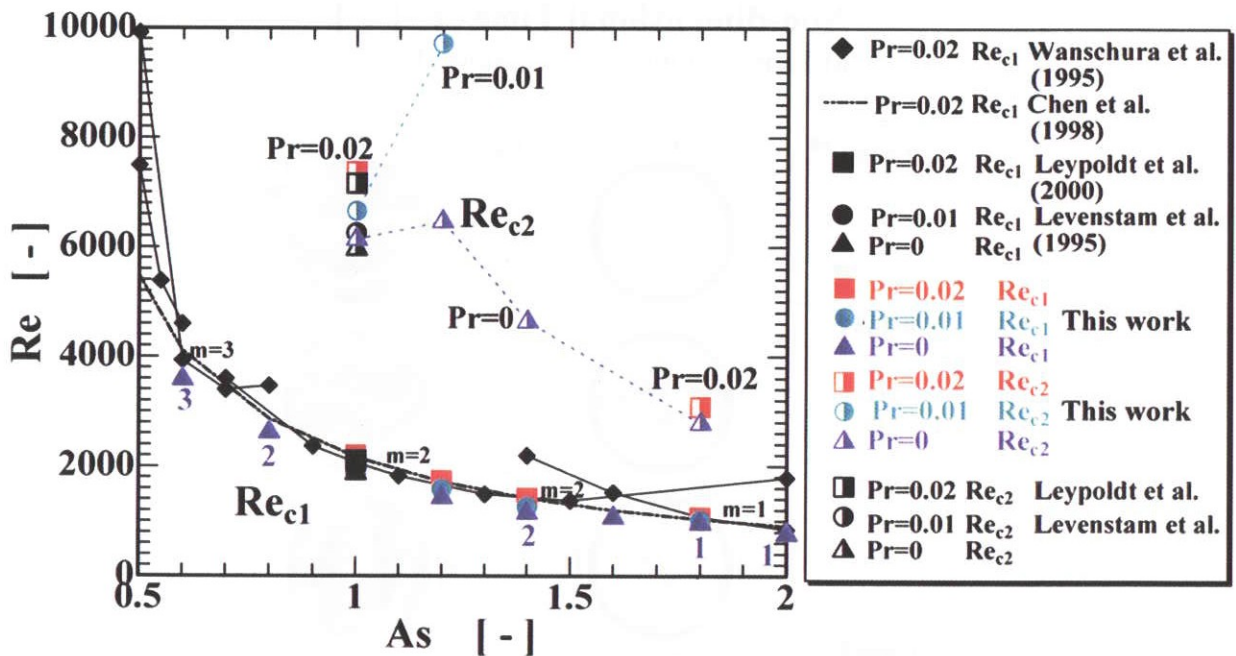


Fig. 15 Simulation results of 3D steady Marangoni flow in a liquid bridge of $Pr=0.01$, $As=1.8$, $Ma=20$, $Re=2000$ and $Bi=0$.

- (a) Time evolution of steady flow.
- (b) 3D view of isothermal and iso-pressure surfaces, trajectories of tracers.
- (c), (d), (e) Distributions of temperature, pressure and velocity.

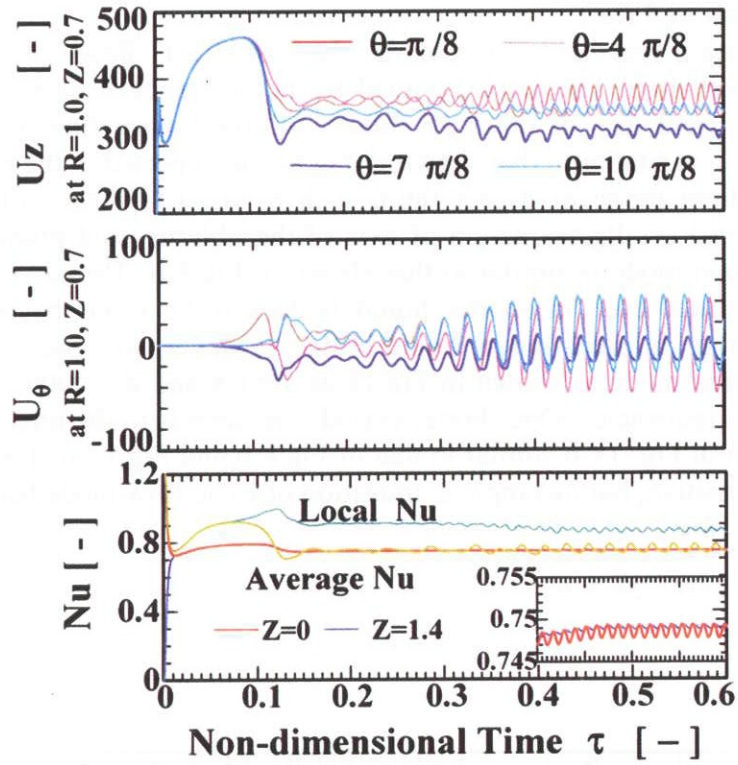
4.2.2 Second transition and Re_{c2}

Beyond a certain threshold value of Re , the steady 3-D flow with $m=2$ becomes unstable and starts oscillation. The second critical Reynolds numbers are plotted in Fig. 16 together with the Re_{c1} and Re_{c2} of other Pr fluids. 3-D oscillatory flow in shorter liquid bridges i.e., $As=1.0-1.2$, is similar to that shown in Fig.8-a, as reported in the previous papers [5,6,8,9]. In the medium range of aspect ratio, such as $As=1.4$, the oscillatory mode is featured by the torsional oscillatory action of axis of the oblique cold plume as shown in Fig.17-b. The oscillation mode is similar to that shown in Fig.8-b. The torsional oscillatory motion becomes dominant even in shorter liquid bridges if Re is far beyond the second critical Reynolds number. In much longer liquid bridge, however, we observed an evolution of an unusual oscillation mode as shown in Fig.18 at $As=1.8$ and $Re=4000$. The oscillation has two characteristic frequencies. One shorter period corresponds to the torsional oscillation of $m=2$ flow as shown in Fig. 18-b similar to that of Fig.8-b and Fig.17-b. The longer period corresponds to an alternative, but incomplete, transition of basic flow mode between $m=2$ and $m=1$, as shown in Fig.18-c.

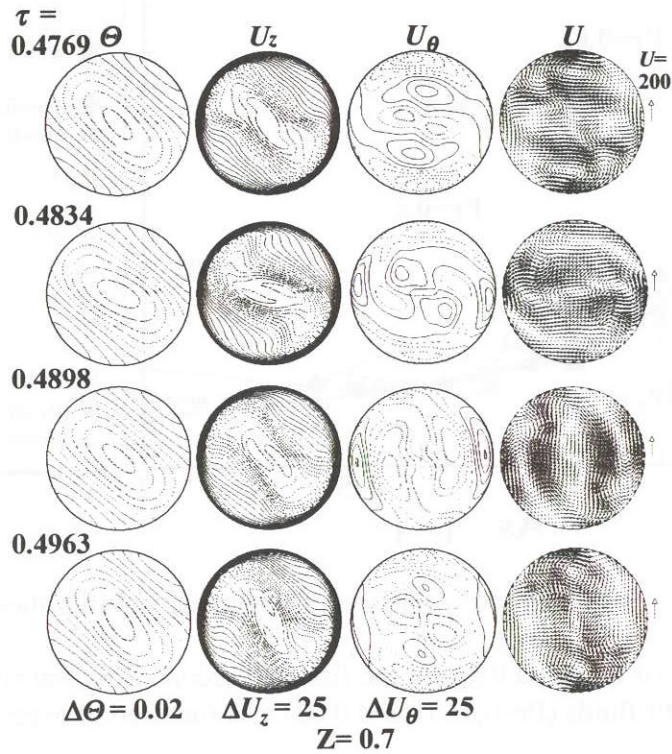


Lines : Re_{c1} for $Pr=0.02$ by linear stability theory by [3] and [4]

Fig. 16 Summary of Re_{c1} and Re_{c2} for the first and second flow transitions in liquid bridge of low Pr fluids ($Pr=0, 0.01$ and 0.02) as a function of aspect ratio, As .

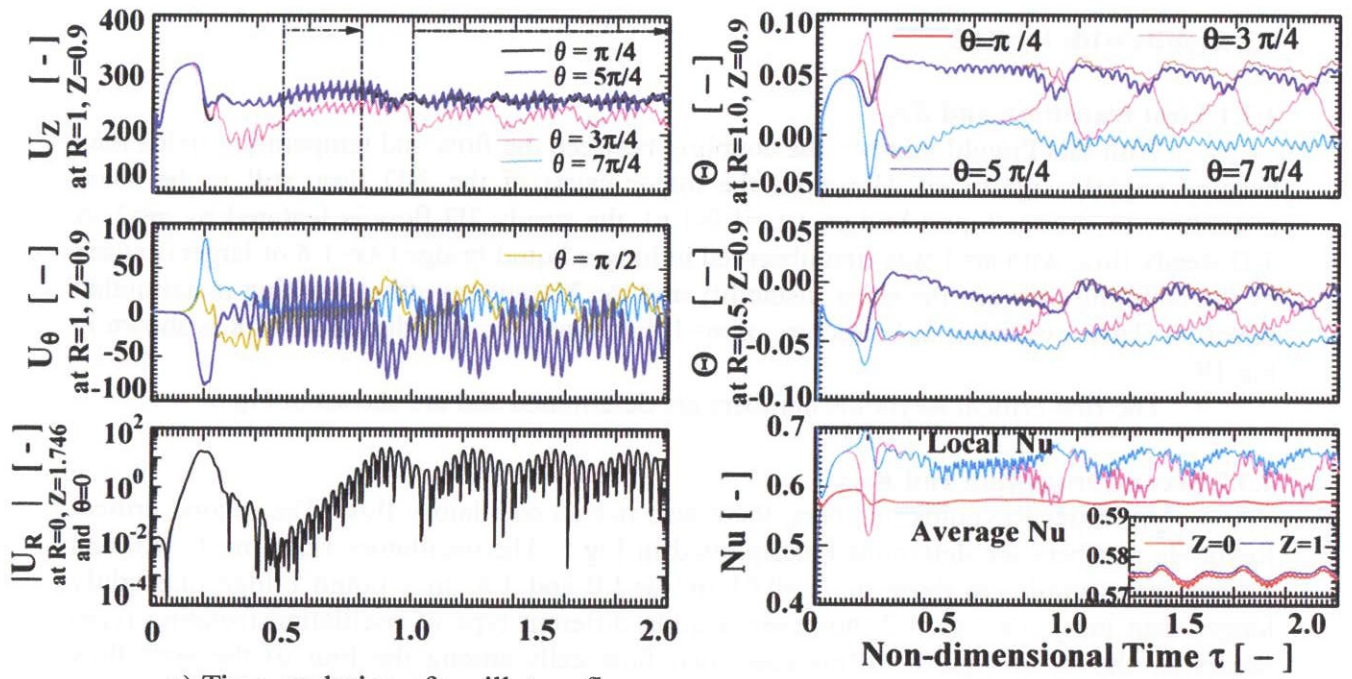


a) Time evolution of oscillatory flow

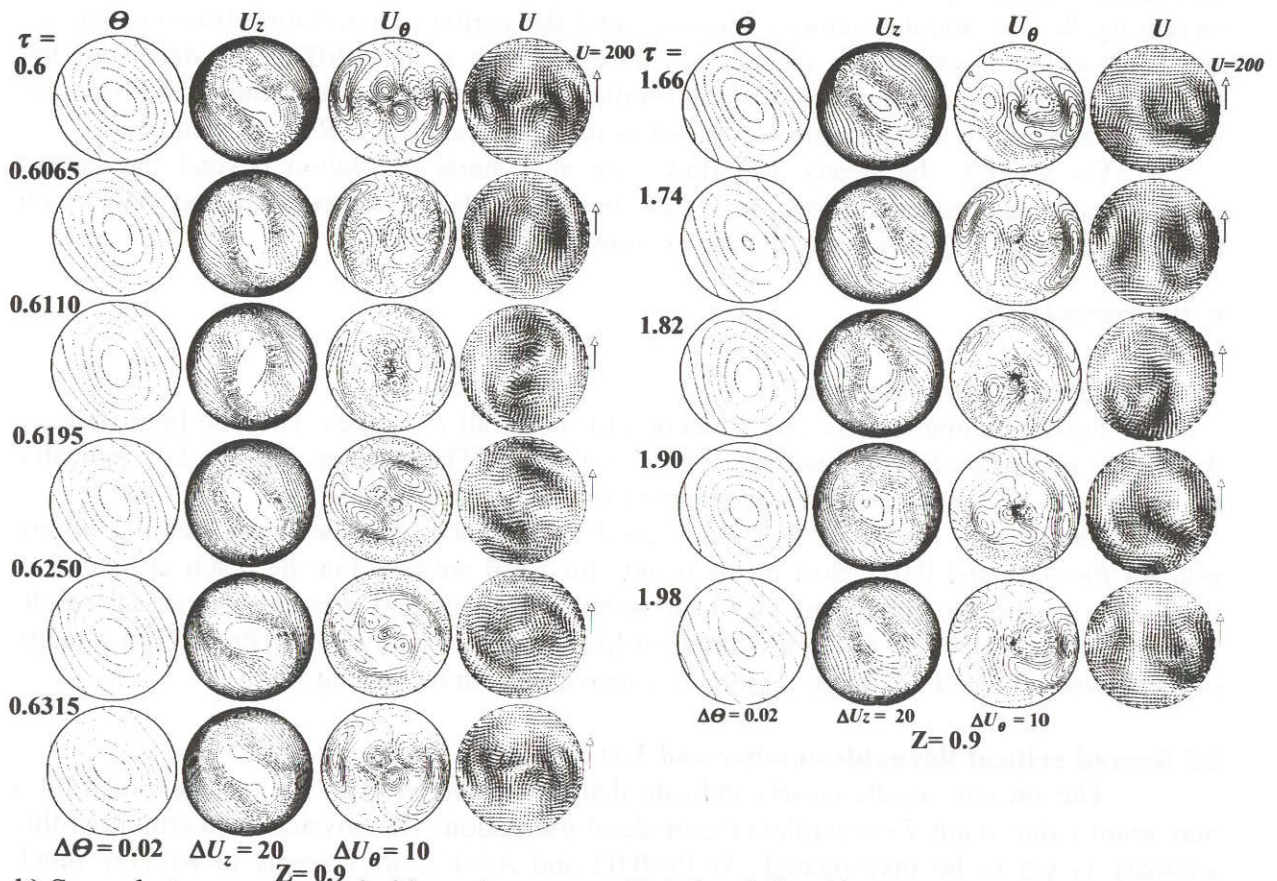


b) Snap-shots of temperature, axial, azimuthal velocity and vectors on $Z=0.7$ plane.
(At $\tau=0.4995$, goes back to $\tau=0.4769$)

Fig. 17 Oscillatory Marangoni flow in liquid bridge of $Pr=0.01$ fluid with $As=1.4$ at $Re=6500$.



a) Time evolution of oscillatory flow.



b) Snap shots over one period in early stage, at $Z=0.9$

c) Snapshots over one longer period in final stage, at $Z=0.9$

Fig. 18 3-D oscillation in a liquid bridge of $Pr=0.01$, $As=1.8$, $Ma=40$, $Re=4000$ and $Bi=0$.

4.3 Results with $Pr=0.02$

4.3.1 First transition and Re_{c1}

With this Prandtl number, the coupling between the flow and temperature fields may become slightly significant. However, the major cause of the 3-D flow still is the shear instability. In shorter liquid bridges ($As=1.0-1.6$), the steady 3D flow is featured by $m=2$. A 3-D steady flow with $m=1$ was first observed in longer liquid bridge ($As=1.8$ or larger) caused by the coupling between the shear instability and the Marangoni effect working in azimuthal direction. Time evolution and structure of $m=1$ disturbance in a bridge of $As=1.8$ is shown in Fig.19.

The first critical Reynolds numbers are determined and are shown in Fig.5.

4.3.2 Second transition and Re_{c2}

At larger Reynolds numbers, there also occurs oscillatory flow. The second critical Reynolds numbers are determined and plotted in Fig.5. The oscillatory flows in $As=1.0$ and 1.4 are quite similar to those of $Pr=0.01$ in $As=1.0$ and 1.4 . In a liquid bridge of slightly longer than unity, i.e., $As=1.2$, however, a quite different type of oscillation (rotating type) occurs as shown in Fig.20. In this case, two flow cells among the four of the $m=2$ flow structure, cf. the four equal sized flow units in Fig.15, become slightly larger than the other two (see Fig.21) and the whole flow and temperature fields starts azimuthal rotation with very small angular velocity. This rotating oscillation is quite different from the rotational oscillation caused by the hydrothermal wave type instability in $Pr=1$ fluid [8,12]. By increasing Re , the angular velocity increases and the period of oscillation becomes shorter and the oscillation amplitudes increase. In these cases, it is very difficult to determine the second critical Reynolds number at which oscillatory flow starts, because the period becomes very long and amplitudes become very small near the second critical Reynolds number.

For $As=1.8$, the steady 3-D flow with $m=1$ starts oscillation beyond the second critical Reynolds number as shown in Fig.22. In this oscillation, temperature and velocity on the mid plane ($Z=0.9$) changes with time as shown in Fig.23.

5. DISCUSSIONS

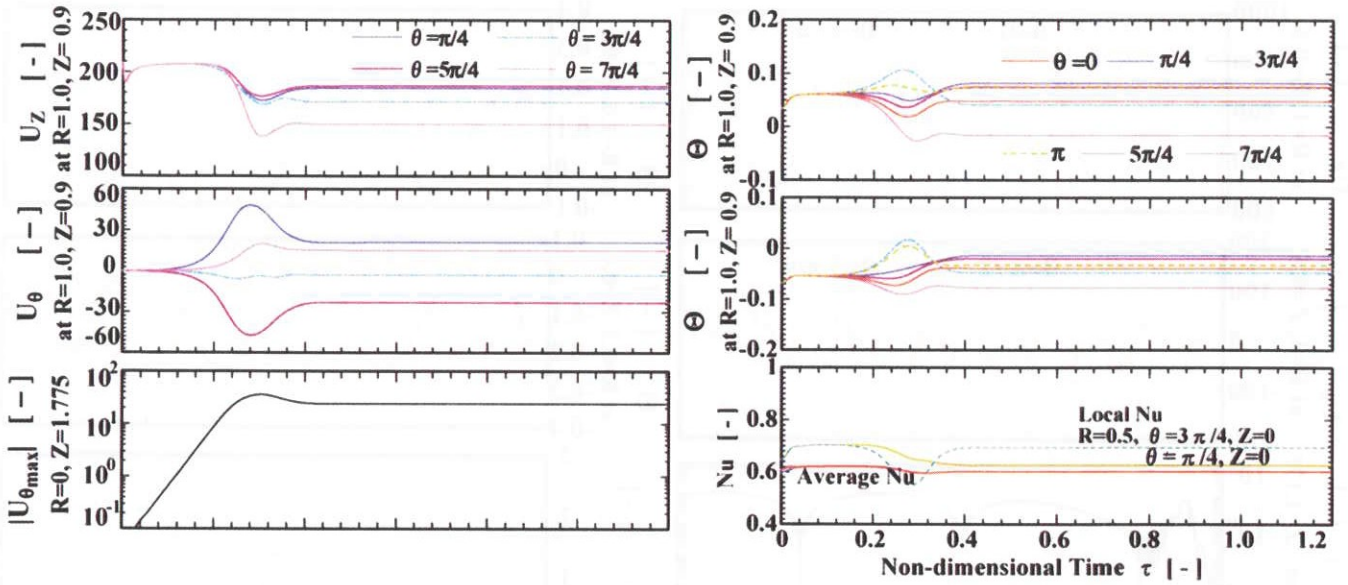
5.1 First critical Reynolds number

Fig.11 summarizes Re_{c1} as a function of As for all Pr values. The thin lines indicate the results of linear stability analyses for $Pr=0.02$ [3,4]. The number near the key indicates the value of m i.e., the azimuthal wave number of the 3-D steady flow.

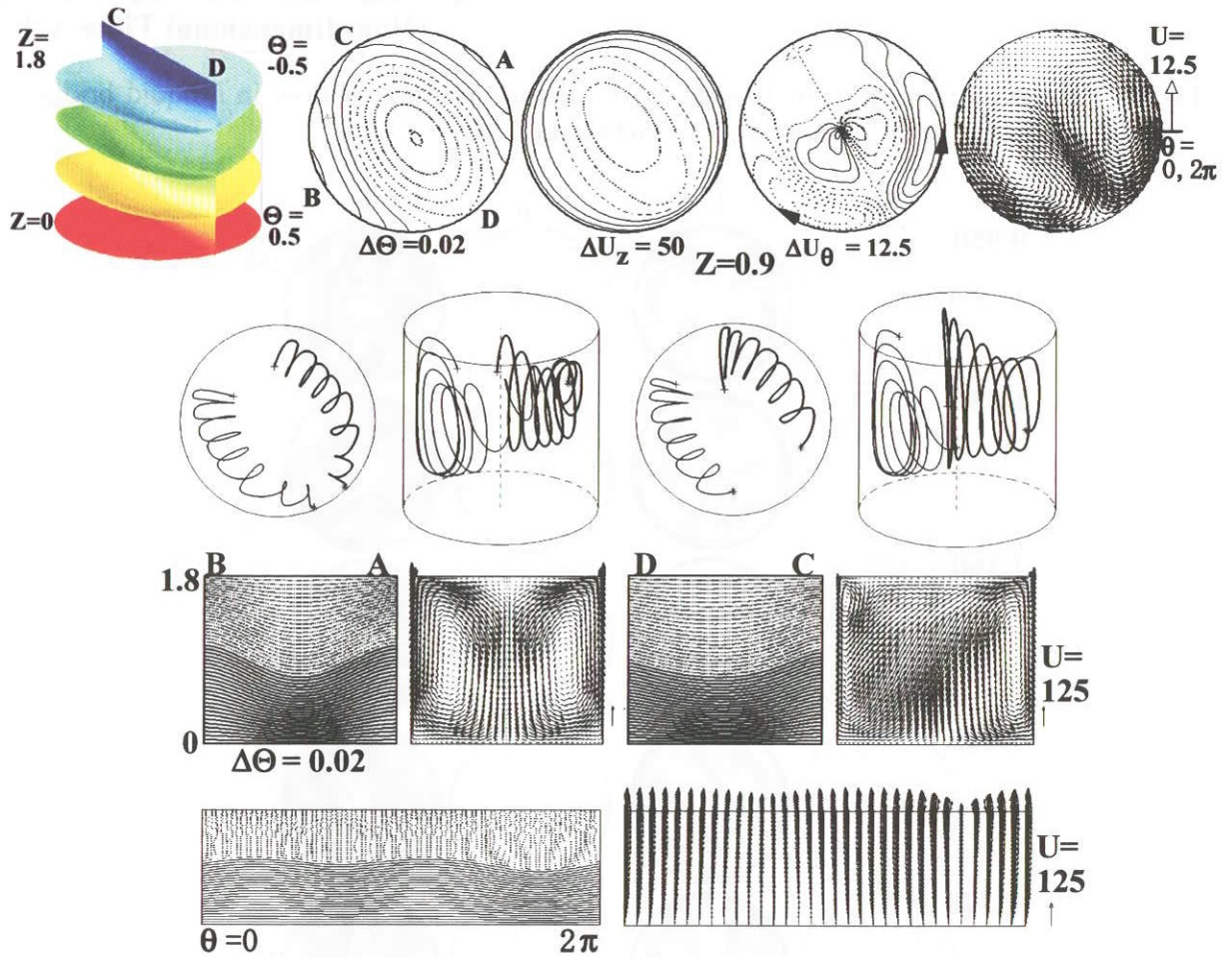
The present results of Re_{c1} show good coincidence with the linear stability within 6%, for $Pr=0.01$ and 0.02 . Most of the results for $Pr=0$ are new but the result at $As=1.0$ is very close to the Re_{c1} predicted by linear stability analysis and previous numerical result. Present results with $Pr=0$ fall below those of linear stability analyses for $Pr=0.02$ in a range of As between 0.6 and 2.0 . In all region, Re_{c1} increases with increasing Pr .

5.2 Second critical Reynolds number and 3-D oscillation mode

The present results clearly indicate that, at around $As=1.2$, Re_{c2} tends to exhibit a maximum value at any Pr regardless the mode of oscillation. The physical background of this anomaly is yet to be investigated. At $Pr=0.02$ and $As=1.2$, Re_{c2} seems to be very much increased. However, there is no reliable method to determine the Re_{c2} for the peculiar oscillatory flow encountered in case of $Pr=0.02$, $As=1.2$. For Re_{c1} and Re_{c2} , complete map is required to understand the features of oscillatory Marangoni convection in liquid bridge of low Prandtl number fluids.



a) Time evolution of oscillatory flow



b) 3D view of isothermal surfaces, trajectories of trace. Distributions of temperature and velocity.

Fig. 19 Time evolution and structures of 3D steady Marangoni flow in $Pr=0.02$ fluids with $As=1.8$, $Ma=50$, $Re=2500$ and $Bi=0$.

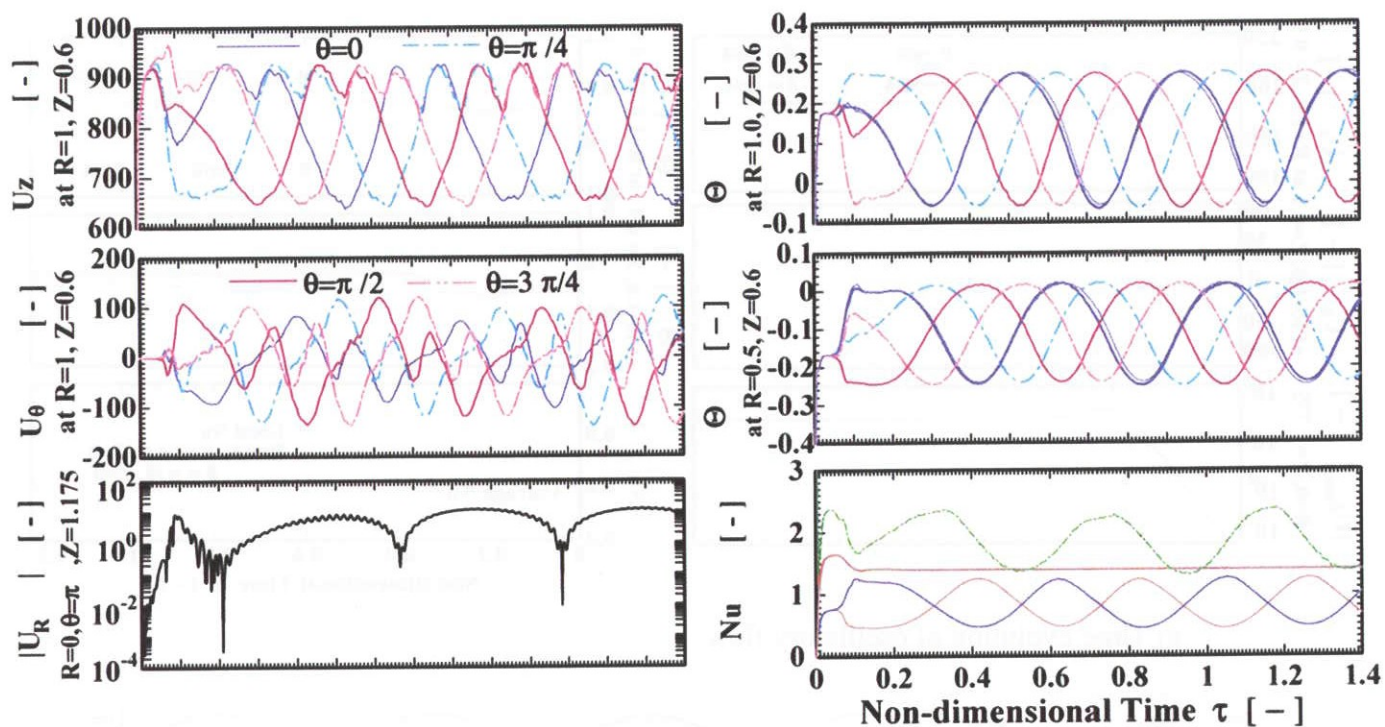


Fig.20 Time evolution of a slowly rotating oscillatory Marangoni flow in a liquid bridge of $Pr=0.02$ fluid with $As=1.2$, $Ma=500$, $Re=25000$ and $Bi=0$

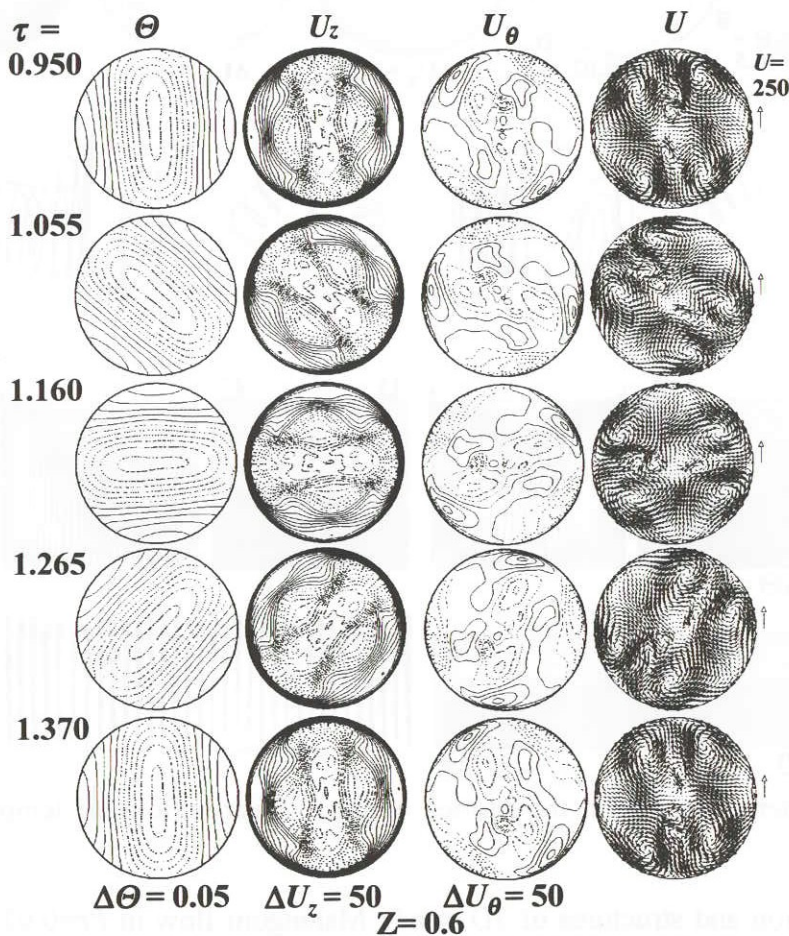


Fig. 21 Snap shots of temperature, axial and azimuthal velocity contours and velocity vectors at $Z=0.6$ over a half period of the rotating oscillation: conditions: see Fig. 20.

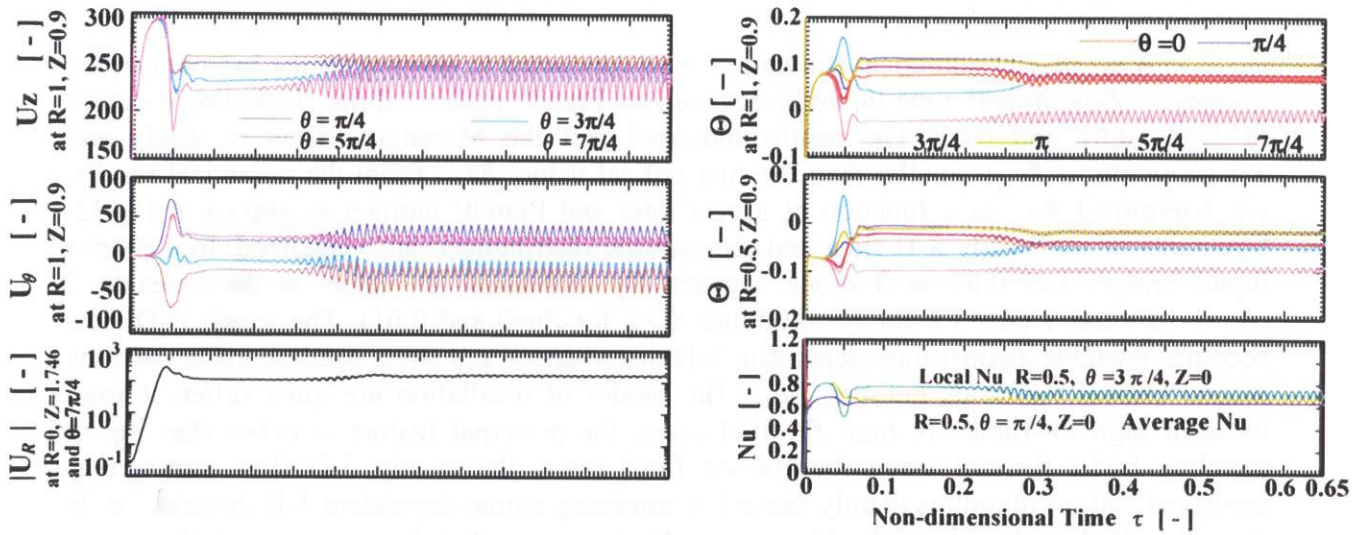


Fig.22 Time evolution of oscillatory Marangoni flow in a liquid bridge of $Pr=0.02$ fluid with $As=1.8$, $Ma=80$, $Re=4000$ and $Bi=0$.

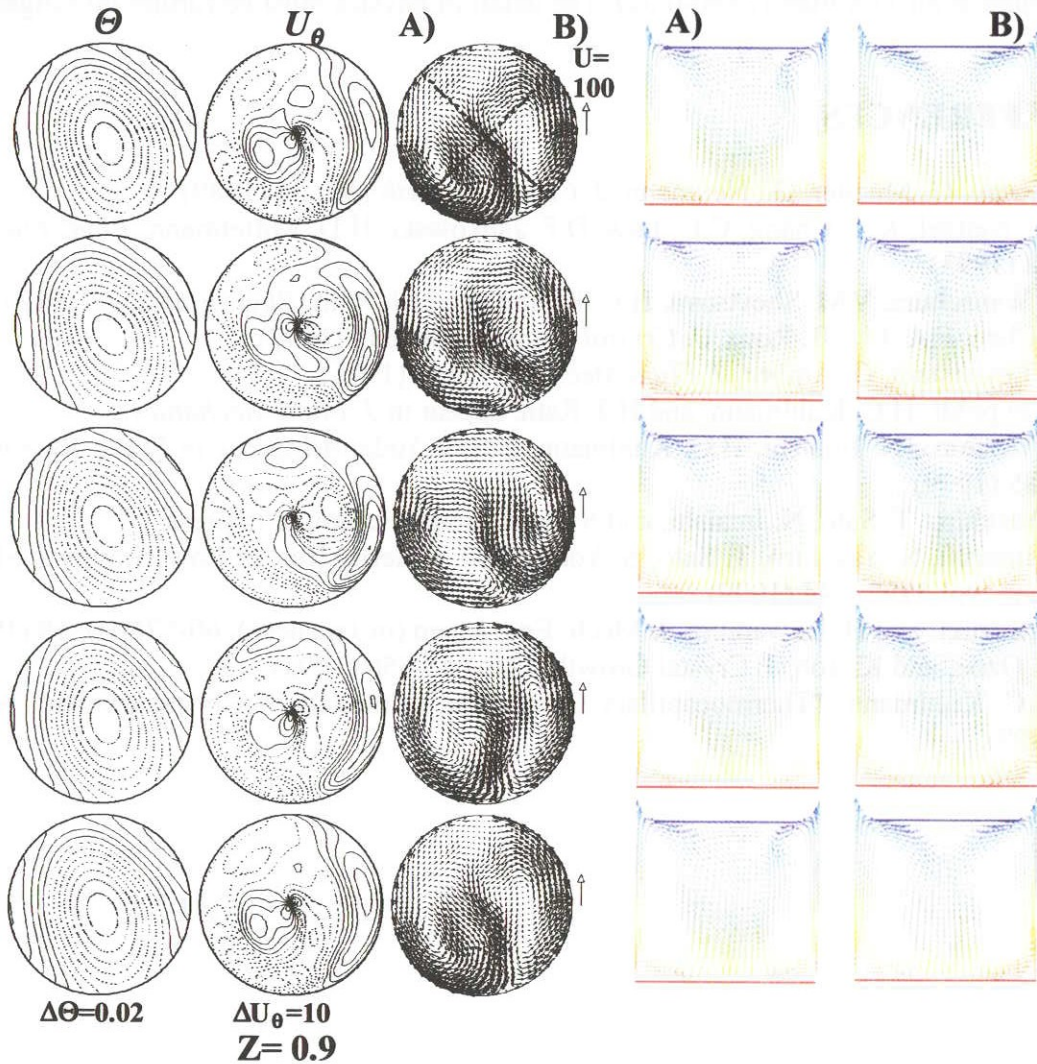


Fig. 23 Snap shots of temperature, azimuthal velocity contours and velocity vectors at $Z=0.9$ and velocity vectors in two vertical planes: conditions : see Fig. 22.

6. CONCLUSION

A set of 3-D numerical simulations was conducted to investigate the behavior of the Marangoni flow in half-zone liquid bridges of low Prandtl number fluids, including the limit of $Pr=0$, 0.01 and 0.02. The results indicated that the Marangoni flow is steady and axisymmetric, if Re is smaller than the first critical value, Re_{c1} . From the numerical results, we determined Re_{c1} as a function of aspect ratio and Prandtl number as shown in Fig.12. Structures of the steady 3-D flow and temperature distributions are visualized. In a shorter liquid bridges ($As=0.6$), $m=3$ mode appears. By increasing As value, m decreases to 2 ($As=1-1.6$) and 1 ($As>1.8$ for $Pr=0.02$ and $As>2$ for $Pr=0$ and 0.01). The steady 3-D flow becomes unstable against time-dependent 3-D disturbances and starts oscillations beyond the second critical Reynolds number, Re_{c2} . The modes of oscillation are quite different from those of high Pr fluids. In high Pr fluid cases, the principal feature is either standing or traveling hydro-thermal wave. In low Pr fluid cases, the steady 3-D flow structure is preserved and oscillation is mainly caused by imposing a time-dependent 3-D disturbance. In these low Pr liquid bridges, the Marangoni effect in azimuthal direction takes little (or no) role. But the coupling between temperature and velocity fields brings up some curious oscillation behavior. At some range of As , the second critical Reynolds number indicates maximum at all Pr values ($Pr=0-0.02$). The detail of physics must be further investigated.

7. REFERENCES

- 1) R. Rupp, G. Mueller, G., Neumann, *J. Crystal Growth*, **97**, 34 (1989)
- 2) G.P. Neitzel, K.T. Chang, C.C. Law, D.F. Jankowski, H.D. Mittelmann, *Phys. Fluids*, **A5**, 108 (1993)
- 3) M. Wanschura, V.M. Shevtsova, H.C. Kuhlmann, H.J. Rath, *Phys. Fluids*, **A7**, 912 (1995)
- 4) G. Chen, F.A. Liz, B. Roux, *J. Crystal Growth*, **180**, 638 (1997).
- 5) M. Levenstam, G. Ambrg, *J. Fluid Mech.*, **297**, 357 (1995)
- 6) J. Leyboldt, H.C. Kuhlmann, and H.J. Rath, appear in *J. Fluid Mechanics*
- 7) S. Yasuhiro, N. Imaishi, H.C. Kuhlmann, and S. Yoda, *Advances in Space Research*, **24**, 1385 (1999)
- 8) S. Yasuhiro, T. Sato, N. Imaishi, and S. Yoda, *Space Forum*, **6**, in press
- 9) N. Imaishi, S. Yasuhiro, T. Sato, S. Yoda, *Proc. Material Res. in Low Gravity 2 SPIE Int. Symp.* vol.3792, 344 (1999)
- 10) T. Suzuki, and H. Kawamura, *J. Mech. Eng. Japan* (in Japanese), **60-578(B)**, 58 (1994)
- 11) H. Ozoe, and K. Toh, *J. Crystal Growth*, **130**, 645-656 (1993).
- 12) H.C. Kuhlmann, "Thermocapillary Convection in models of Crystal growth", Springer (1999)